Efficient Total Variation Algorithm for Fetal Brain MRI Reconstruction

Sébastien Tourbier[1,2], Xavier Bresson[1,2], Patric Hagmann[2], Jean-Philippe Thiran[3,2], Reto Meuli[2], and Meritxell Bach Cuadra[1,2,3,⋆]

[1] Centre d'Imagerie Biomédicale, Switzerland
[2] Department of Radiology, Lausanne University Hospital Center (CHUV) and University of Lausanne (UNIL), Switzerland
[3] Signal Processing Laboratory (LTS5), Ecole Polytechnique Fédérale de Lausanne (EPFL), Switzerland

Abstract. Fetal MRI reconstruction aims at finding a high-resolution image given a small set of low-resolution images. It is usually modeled as an inverse problem where the regularization term plays a central role in the reconstruction quality. Literature has considered several regularization terms s.a. Dirichlet/Laplacian energy [1], Total Variation (TV)-based energies [2,3] and more recently non-local means [4]. Although TV energies are quite attractive because of their ability in edge preservation, standard explicit steepest gradient techniques have been applied to optimize fetal-based TV energies. The main contribution of this work lies in the introduction of a well-posed TV algorithm from the point of view of convex optimization. Specifically, our proposed TV optimization algorithm for fetal reconstruction is optimal w.r.t. the asymptotic and iterative convergence speeds $O(1/n^2)$ and $O(1/\sqrt{\varepsilon})$, while existing techniques are in $O(1/n)$ and $O(1/\varepsilon)$. We apply our algorithm to (1) clinical newborn data, considered as ground truth, and (2) clinical fetal acquisitions. Our algorithm compares favorably with the literature in terms of speed and accuracy.

1 Introduction

The aim of fetal brain MRI reconstruction is to reconstruct a high-resolution (HR) image X given a set of low-resolution (LR) images X_k^{LR}, which may be highly corrupted with noise, blurring, intensity bias and (large-scale) motion. The fetal reconstruction problem can be cast as an inverse problem s.t. $\min_X \sum_{k=1}^{K} \|H_k X - X_k^{LR}\|^2$, where H_k are supposedly linear operators that transform the HR image X into a LR (corrupted) image X_k^{LR}. The above least square problem is said to be ill-posed, meaning that it has generally no meaningful solutions. The natural solution is to regularize, a la Tikhonov, that is to say (1) making assumptions about the HR image X s.a. smoothness, edge recovery, histogram conservation, etc, and (2) adding a regularization term $R(X)$ that projects X into some spaces that hold the desired properties, i.e.

⋆ This work is supported by Grant SNSF-141283.

P. Golland et al. (Eds.): MICCAI 2014, Part II, LNCS 8674, pp. 252–259, 2014.

$\min_X R(X) + \frac{\lambda}{2} \sum_{k=1}^{K} \|H_k X - X_k^{LR}\|^2$, where λ controls the trade-off between regularization strength and data fidelity.

In the last years, research interest in reconstruction of fetal MRI has grown considerably. In [5], the first reconstruction technique based on slice-to-volume registration and scattered data interpolation was introduced. Later, the same authors have proposed a new method that iterates between motion correction and HR image estimation via edge-preserving regularization [3]. Moreover, they have developed an open-source toolkit (BTK) [4] for fetal brain MR image processing that uses non-local means [6] as image regularization. In [1], the authors introduce an inverse problem for image reconstruction and used the Dirichlet/Laplacian energy as regularization. They have extended their work in [7] to carry out the fetal segmentation problem. Inspired by previous approaches, [2] alternate between motion correction via slice-to-volume registration and image reconstruction through an inverse problem that uses the edge-preserving regularization defined in [8]. Besides, the method incorporates intensity matching and voxel-slice rejection via robust statistics. Finally, in [9,10], authors introduce a rather different approach based on slice intersection motion correction combined with a gradient-weighted averaging technique for image estimation. They further improved their technique in [11] within a unified formulation.

Given the literature, the most accepted image acquisition model is a linear model designed as: $X_k^{\mathrm{LR}} = L_k G_k B_k M_k X + n_k$, where X is the HR image, X_k^{LR} is a low-resolution (LR) image acquired by the MR scanner, M_k is a motion operator, L_k is a down-sampling operator, G_k is a blurring operator, B_k is a bias operator and n_k is an additive Gaussian noise. In the rest of the paper, we denote $H_k := L_k G_k B_k M_k$. The most generic reconstruction algorithm consists in iterating the following two steps until convergence:
Step 1: Motion estimation $M_k^{m+1} = \arg\min_{M_k} \sum_k \|L_k G_k B_k M_k X^m - X_k^{\mathrm{LR}}\|^2$,
Step 2: Image recovery $X^{m+1} = \arg\min_X \; R(X) + \frac{\lambda}{2} \sum_k \|L_k G_k B_k M_k^{m+1} X - X_k^{\mathrm{LR}}\|^2$, where $R(X)$ is the regularization term. The main contribution of this work lies in the design of a fast, accurate and guaranteed-to-converge algorithm for the fetal reconstruction problem that is based on the Total Variation (TV) energy (Section 2). We will validate our reconstruction algorithm in two ways: (1) we will confirm numerically the theoretical speed of convergence and (2) we will carry out tests on clinical datasets (Section 3). We will also compare the proposed algorithm to NLM embedded in the BTK toolbox [4], and will show that it compares favorably in terms of speed and accuracy.

2 High-Resolution Reconstruction with Total Variation and Convex Optimization

We consider the following discrete setting. Let S_X, S_Y be two finite-dimensional real vector spaces with inner product $\langle \cdot, \cdot \rangle$, norm $\| \cdot \| := \langle \cdot, \cdot \rangle^{1/2}$, dim $S_X = n$ where n is the total number of pixels/voxels and dim $S_Y = m = n \cdot d$ where $d = \{2, 3\}$ for 2D/3D images. Let high-resolution (HR) images $X \in S_X$ and $DX \in S_Y$ their gradients. The gradient operator $D : S_X \to S_Y$ is a continuous

linear operator with norm $\|D\| := \max\{\|DX\| \mid X \in S_X,\ \|X\| \leq 1\}$. The fetal reconstruction problem can be formulated as a first order convex optimization problem:

$$\min_{X \in S_X} \|X\|_{TV} + \frac{\lambda}{2} \sum_{k=1}^{K} \|H_k X - X_k^{LR}\|^2 \quad \text{s.t.} \quad X \geq 0 \tag{1}$$

where $\|X\|_{TV} := \|DX\|$ is the TV semi-norm [12]. Minimizing problem 1 is a convex but non-smooth optimization problem. Non-smooth minimization has been challenging since the introduction of TV in imaging problems in the 90's. The most common methodology that optimizes TV consists in using a smooth ε-regularization of TV s.t. $\|X\|_{TV_\varepsilon} := \sum_{i,j} \sqrt{|\nabla X_{i,j}|^2 + \varepsilon} \ \rightarrow \ \|X\|_{TV}$ for $\varepsilon \to 0$. The natural main motivation to introduce a quadratic approximation of TV is to apply smooth optimization tools like gradient descent or conjugate gradient schemes. In the context of fetal reconstruction, this approach was considered with $\varepsilon = 1$ in [2,3] based on the edge-preserving technique introduced in [8]. In [1], the authors considered large ε that links to the Dirichlet/Laplacian energy, i.e. $\|X\|_{TV_\varepsilon} \to \|X\|_{Dir} = \|DX\|^2$ for $\varepsilon \to \infty$. Standard optimization techniques for ε-TV have been carried out with the calculus of variation followed by an explicit steepest gradient descent scheme, such as in [2,3]. However, the standard PDE-based optimization scheme is slow because it is restricted by the Courant-Friedrichs-Lewy's condition, that basically set an upper bound on the time step of the iterative flow s.t. $\Delta t \leq \varepsilon \Delta x / \max_{i,j} EL_{i,j}$, where EL corresponds to the Euler-Lagrange equations (speed of the flow) and Δx is the spatial step. It is well-known that the asymptotic rate of convergence of steepest descent techniques for smooth energy is $O(1/n)$ where n is the iteration step and the iterative rate is $O(1/\varepsilon)$, see e.g. [13]. Besides the speed, there are two other limitations with ε-TV: (1) the TV term is not exactly solved because we compute an ε-solution, which does not preserve as well image contrasts and small-scale structures as the exact TV, and (2) there is an extra parameter, ε, to select (unlike exact TV).

Our main objective is to develop a fast and accurate optimization scheme for TV-based fetal reconstruction problems. In the last five years, fast TV-based optimization algorithms based on convex optimization theory have been developed to solve the sparse reconstruction problem a.k.a. compressed sensing. In this work, we will use an accelerated primal-dual hybrid gradient (PDHG) method based on [14] to design a fast algorithm that offers accurate solutions and is guaranteed to converge to a global solution for 1 (i.e. solution is independent of the initialization). We rewrite 1 as the saddle point problem or equivalently as a primal-dual optimization problem

$$\min_{X \in S_X} \max_{P \in S_Y} \langle \nabla X, P \rangle + G(X) + \delta_C(X) - F^\star(P) \tag{2}$$

with $G(X) = \frac{\lambda}{2} \sum_k \|H_k X - X_k^{LR}\|^2$, the convex function $F^\star$ denotes the barrier function of the ℓ_∞ unit ball, that is $F^\star(P) = 0$ if $|P_i| \leq 1$ for $1 \leq i \leq n$, otherwise $F^\star(P) = +\infty$ and $\delta_C(X)$ is a barrier function of the convex set $C :=$

$\{X \geq 0\}$. As G is uniformly convex, we may therefore apply [14] to solve 2. The proposed algorithm consists in iterating

$$\begin{aligned}
P^{n+1} &= \text{prox}_{\sigma^n F^\star}(P^n + \sigma^n D\bar{X}^n) \\
X^{n+1} &= \text{prox}_{\tau^n G + \delta_C}(X^n - \tau^n D^t P^{n+1}) \\
\theta^{n+1} &= 1/\sqrt{1 + 2\rho\tau^n}, \quad \tau^{n+1} = \theta^{n+1}\tau^n, \quad \sigma^{n+1} = \sigma^n/\theta^{n+1} \\
\bar{X}^{n+1} &= X^{n+1} + \theta^{n+1}(X^{n+1} - X^n)
\end{aligned}$$

where $\text{prox}_E(X) := \arg\min_Y \; E(Y) + \frac{1}{2}\|Y - X\|^2$. Solution of the inner problem 2 is given by $(\text{prox}_{\sigma^n F^\star}(Z))_i = Z_i / \max\{1, |Z_i|\}$ where $Z = P^n + \sigma^n D\bar{X}^n$. The solution of the least-square problem 2, $\min_{X \geq 0} \; \frac{\lambda}{2}\sum_k \|H_k X - X_k^{LR}\|^2 + \frac{1}{2\tau^n}\|X - W\|^2$ with $W = X^n - \tau^n D^t P^{n+1}$ can be computed with several approaches. We use a semi-implicit gradient descent scheme that provides fast good approximate minimizing solutions. More specifically, the Euler-Lagrange solution of 2 is $\lambda\tau^n(HX - X^{LR}) + X - W = 0$ where $H := \sum_k H_k^t H_k$ and $X^{LR} := \sum_k H_k^t X_k^{LR}$ (note that H and X^{LR} are computed only once) and the iterative semi-implicit scheme is defined as $X^{l+1} = \mathcal{P}_C(X^l - \Delta t\lambda\tau^n(HX^l - X^{LR}) + \Delta t W)/(1 + \Delta t)$ where $\mathcal{P}_C$ is the projection operator onto the set $X \geq 0$ and $\Delta t = 0.1$ in all experiments.

Algorithm 2-2 is guaranteed to converge to a saddle point to 2 and therefore a solution of the fetal reconstruction problem 1 as long as the initial time steps are chosen to be $\sigma^0\tau^0 \leq 1/\|D\|^2$, see [14] for more details. More importantly, the asymptotic speed of convergence of the algorithm is quadratic, i.e. $O(\frac{1}{n^2})$, which is actually optimal for this class of problems as proved by Nesterov in [15]. In other words, the proposed TV optimization algorithm is expected to be faster than the TV-based algorithms published in the literature for fetal reconstruction.

Numerical Experiment. We carry out a numerical experiment to validate the theoretical asymptotic rate of convergence and also the iterate rate of convergence that is expected to be $O(\frac{1}{\sqrt{\varepsilon}})$, see [13]. In order to speed up the experiments, we test our algorithm on a 2D HR fetal image with 4 LR images that are corrupted with noise but with no added motion. Figure 1 reports our numerical result. We test the asymptotic convergence rate for exact TV optimization (the proposed algorithm 2-2) and for ε-TV (using an explicit gradient flow algorithm as in [2,3]). The computed slope of our optimization algorithm, -2.32, is close to the theoretical one, i.e. -2, and slope of ε-TV, -1.42, is also close to the theory, i.e. -1. We also tested the iterative rate of convergence but we do not report the plot here because of the lack of space. The computed slope, -0.30, is also close to the theory, i.e. -0.5. As a summary, this numerical experiment confirms the fast speed and accuracy of the proposed algorithm.

3 Experiments on Clinical Datasets

We carry out quantitative evaluations on *simulated* fetal acquisitions from a newborn data, as performed in [2]. Firstly, we compare the reconstruction quality with respect to (w.r.t.) the number of LR images. Secondly, we perform a leave-one-out analysis on the same dataset. Eventually, we qualitatively evaluate the proposed algorithm on healthy and pathological fetal MRIs. Results are

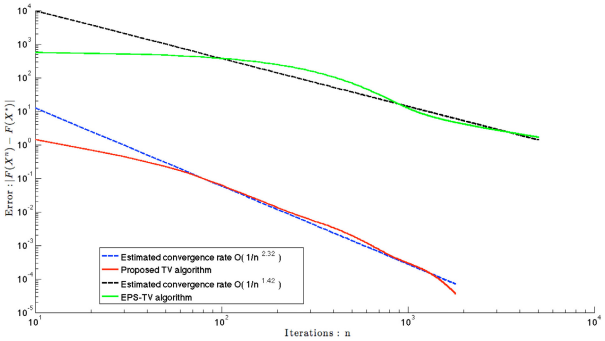

Fig. 1. Numerical experiment to test the asymptotic rate of convergence for exact and ε-TV optimization algorithms for fetal image reconstruction.

compared with the algorithm proposed in the open-source toolbox BTK [4]. Our method is implemented in C++ with Insight Toolkit [16] and tests are run on a 3.4 GHz Quadcore i7-3770 CPU. Estimation of the motion parameters and computation of the matrices H_k (adjusted to fit our acquisition setting) in 1 are performed with BTK. Global rigid stack registration is used for the ground-truth dataset (Section 3.1). Global rigid stack registration followed by slice-to-volume registration is employed in the case of the clinical datasets (Section 3.2). Parameters are optimized for both BTK and our algorithm. Their values are selected to have the best reconstructed HR image in the sense of the highest Peak-Signal-To-Noise Ratio (PSNR) when the ground-truth image is known, or with the most similar within-tissue contrast to the original LR images.

3.1 Ground-Truth Dataset

To simulate the acquisition of fetal brain MRI, we employ a T2-weighted TurboFLASH image of a mature newborn. The image was acquired on a 3T Siemens Tim Trio with $TR = 4000ms$, $TE = 3.7ms$, slice thickness of $1.2mm$ and in-plane resolution of $0.78mm$. We consider the ground-truth image as the original image that was bias field corrected [17] and isotropically interpolated to a resolution of $1mm$ using B-splines. Nine LR images, three per acquisition direction, with in-plane resolution of $1mm$, slice thickness of $3mm$, were simulated from the ground-truth image by applying downsampling and blurring operations. Note that $1mm$ shifts were also introduced for images with the same acquisition direction. Similarly to [3], no motion was added as we want to evaluate the proposed algorithm in terms of image recovery quality in ideal conditions. Ground truth data and a simulated LR image are illustrated at the top of Figure 2. We assess the performance of our algorithm w.r.t. the LR images by randomly selecting $1, 2, \ldots, 9$ LR images as in [3] and repeat the experiment 10 times. The reconstruction quality was evaluated with the PSNR averaged over all experiments. Results are presented in Figure 2(d). We observe that the reconstruction quality

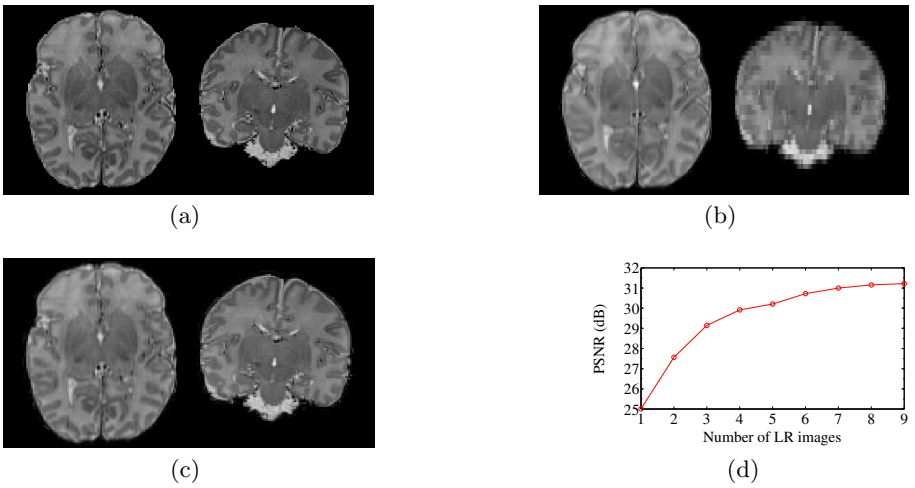

Fig. 2. Simulated Dataset; a) Newborn ground-truth volume. b) simulated transversal LR image. c) TV reconstruction using 9 LR images. d) Reconstruction quality (PSNR) w.r.t. the number of LR images.

improves as the number of LR images increases, as reported in [3]. This experiment also confirms a result from [3], i.e. the performance of the reconstruction algorithm marginally improves when more than 4-5 LR images are used.

Leave-one-out Analysis. We also assess the performance of our algorithm with a leave-one-out analysis, as in [2], carried out on a set of 6 LR images (2 LR images in each acquisition direction). In this experiment, only 5 volumes are used for the reconstruction and the ground-truth is considered to be the left LR image. This situation is close to a clinical setting, where only 3 to 6 volumes can usually be exploited. We compute the normalized root mean square error (NRMSE) and the running time. Table 1 shows that our TV algorithm performs a bit better in terms of reconstruction quality and speed. We also notice that BTK uses a parallel implementation of the non-local means algorithm, while the proposed TV algorithm has no such speed-up here. Future parallel implementation of TV optimization may drastically reduce the presented computational time.

Table 1. Results of the leave-one-out analysis using 6 LR volumes of the simulated dataset

	BTK algorithm	Proposed TV algorithm
NRMSE	0.0466 ± 0.0066	0.0451 ± 0.0067
Running time (sec.)	251.3 ± 2.7	231.7 ± 7.4

3.2 Fetal Datasets

Fetal brain MR images were acquired on a 1.5T Siemens Aera using a T2-weighted HASTE sequence (TE/TR = 90/1200 ms.) with resolution $1.125 \times 1.125 \times 3.6mm^3$. Data set is composed of one healthy brain H1 (25 GA) and one pathological brain P1 (22 GA) diagnosed with complete agenesis of the corpus callosum and cephalic disorder. The acquisition for fetuses H1 and P1 consists respectively of a set of 6 and 4 stacks, where at least one stack is available in each anatomical direction. Reconstruction results are illustrated in Figure 3.

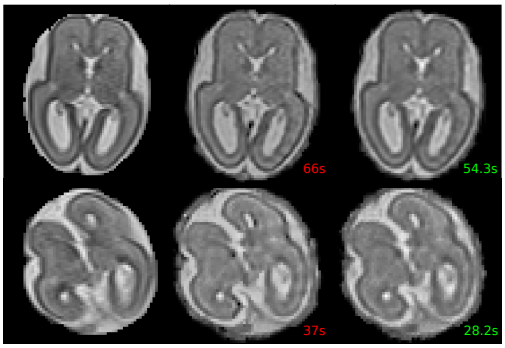

Fig. 3. HR brain reconstruction of clinical fetal datasets. Rows: transversal view of H1 and P1, respectively; First column: 2D slice of LR image; Second column: BTK reconstruction; Third column: TV reconstruction; Running time is reported in the corner of each image; Intensity normalization was used for improved visualization.

Qualitative evaluations on both healthy and pathological brains show that the algorithm is well adapted to clinical scenarios. We observe that TV reconstruction tends to better preserve intensity and within-tissue contrast, which is essential for subsequent computer-aided diagnosis. Extensive quantitative tests will be performed to evaluate the algorithm in multiple clinical conditions.

4 Conclusion

In conclusion, the proposed TV reconstruction algorithm for fetal brain MRI shows great promise in terms of accuracy and speed for clinical datasets. The long-term objective is to develop from the proposed optimization technique more sophisticated fetal reconstruction techniques such as non-local TV [18], inverse TV scale space [19] and higher order TV [20].

References

1. Gholipour, A., Estroff, J., Warfield, S.: Robust Super-Resolution Volume Reconstruction from Slice Acquisitions: Application to Fetal Brain MRI. IEEE TMI 29(10), 1739–1758 (2010)

2. Kuklisova-Murgasova, M., Quaghebeur, G., Rutherford, M., Hajnal, J., Schnabel, J.: Reconstruction of Fetal Brain MRI with Intensity Matching and Complete Outlier Removal. Medical Image Analysis 16, 1550–1564 (2012)
3. Rousseau, F., Kim, K., Studholme, C., Koob, M., Dietemann, J.-L.: On Super-Resolution for Fetal Brain MRI. In: Jiang, T., Navab, N., Pluim, J.P.W., Viergever, M.A. (eds.) MICCAI 2010, Part II. LNCS, vol. 6362, pp. 355–362. Springer, Heidelberg (2010)
4. Rousseau, F., Oubel, E., Pontabry, J., Schweitzer, M., Studholme, C., Koob, M., Dietemann, J.: BTK: An Open-Source Toolkit for Fetal Brain MR Image Processing. Computer Methods and Programs in Biomedicine 109, 65–73 (2013)
5. Rousseau, F., Glenn, O., Iordanova, B., Rodriguez-Carranza, C., Vigneron, D., Barkovich, J., Studholme, C.: A Novel Approach to High Resolution Fetal Brain MR Imaging. In: Duncan, J.S., Gerig, G. (eds.) MICCAI 2005. LNCS, vol. 3749, pp. 548–555. Springer, Heidelberg (2005)
6. Buades, A., Coll, B., Morel, J.: A review of image denoising algorithms, with a new one. SIAM Multiscale Modeling and Simulation (MMS) 4(2), 490–530 (2005)
7. Gholipour, A., Estroff, J., Barnewolt, C., Connolly, S., Warfield, S.: Fetal Brain Volumetry Through MRI Volumetric Reconstruction and Segmentation. International Journal of Computer Assisted Radiology and Surgery 6(3), 329–339 (2011)
8. Charbonnier, P., Blanc-Féraud, L., Aubert, G., Barlaud, M.: Deterministic Edge-Preserving Regularization in Computed Imaging. IEEE TIP 6(2), 298–311 (1997)
9. Kim, K., Habas, P., Rousseau, F., Glenn, O., Barkovich, A., Studholme, C.: Intersection Based Motion Correction of Multi-Slice MRI for 3D in Utero Fetal Brain Image Formation. IEEE Transactions on Medical Imaging 29(1), 146–158 (2010)
10. Studholme, C.: Mapping Fetal Brain Development in utero Using MRI: The Big Bang of Brain Mapping. Review of Biomedical Engineering 13, 345–368 (2011)
11. Fogtmann, M., Seshamani, S., Kim, K., Chapman, T., Studholme, C.: A Unified Approach for Motion Estimation and Super Resolution Reconstruction from Structural Magnetic Resonance Imaging on Moving Subjects. In: Murgasova, M., Rousseau, F., Rueckert, D., Schnabel, J., Studholme, C., Zöllei, L., Gerig, G. (eds.) MICCAI Workshop on Perinatal and Paediatric Imaging, pp. 9–26 (2012)
12. Rudin, L.I., Osher, S., Fatemi, E.: Nonlinear Total Variation Based Noise Removal Algorithms. Physica D 60(1-4), 259–268 (1992)
13. Beck, A., Teboulle, M.: A Fast Iterative Shrinkage-Thresholding Algorithm for Linear Inverse Problems. SIAM J. Imaging Sci. 2(1), 183–202 (2009)
14. Chambolle, A., Pock, T.: A First-Order Primal-Dual Algorithm for Convex Problems with Applications to Imaging. JMIV 40(1), 120–145 (2011)
15. Nesterov, Y.: Smooth Minimization of Non-Smooth Functions. Mathematic Programming 103, 127–152 (2005)
16. Yoo, T.S., Ackerman, M.J., Lorensen, W.E., Schroeder, W., Chalana, V., Aylward, S., Metaxas, D., Whitaker, R.: ITK - The Insight Toolkit. In: Medicine Meets Virtual Reality, pp. 586–592 (2002)
17. Tustison, N., Gee, J.: N4ITK: ITK for MRI Bias Field Correction (2009)
18. Gilboa, G., Osher, S.: Nonlocal Operators with Applications to Image Processing. SIAM Multiscale Modeling and Simulation (MMS) 7(3), 1005–1028 (2007)
19. Osher, S., Burger, M., Goldfarb, D., Yin, W.: An Iterative Regularization Method for Total Variation-based Image Restoration. SIAM MMS 4, 460–489 (2005)
20. Wu, C., Tai, X.: Augmented Lagrangian Method, Dual Methods, and Split Bregman Iteration for ROF, Vectorial TV, and High Order Models. SIAM SIIMS 3(3), 300–339 (2010)